Journal of Hazardous Materials 175 (2010) 151–158

Contents lists available at ScienceDirect

Journal of Hazardous Materials

journal homepage: www.elsevier.com/locate/jhazmat

Tyre char preparation from waste tyre rubber for dye removal from effluents

Edward L.K. Mui, W.H. Cheung, Gordon McKay*

Department of Chemical and Biomolecular Engineering, Hong Kong University of Science and Technology, Clear Water Bay, Kowloon, Hong Kong

ARTICLE INFO

Article history:
Received 10 June 2009
Received in revised form
28 September 2009
Accepted 28 September 2009
Available online 2 October 2009

Keywords:
Tire
Char
Adsorption
Organics
Isotherm

ABSTRACT

A number of chars from waste tyre rubber were prepared by carbonisation at 673–1173 K. The effects of holding time, heating rate and particle size on the textural characteristics and elemental composition of the resultant chars were investigated. It was demonstrated that temperatures over 773 K did not have a significant improvement on the total surface area but resulted in lower char yields following increased aromatisation. Modelling of dye adsorption isotherms showed that the Redlich–Peterson expression yields the best-fit between experimental and predicted data. Furthermore, for a larger sized dye like Acid Yellow 117 (MW = 848 g/mol), the amount adsorbed by the tyre char is not directly proportional to the total surface area when compared with a commercial carbon, revealing that factors other than total surface area are involved in the adsorption potential of the tyre chars.

1. Introduction

It was estimated that the world production of scrap tyres was a total of 1000 million per year [1]. The disposal of waste tyre represents a major environmental issue throughout the world, since the same properties that make them desirable as tyres, most notably durability, also make their disposal and reprocessing difficult, they are almost immune to biological degradation. The major aspects of the problems are listed as follows:

- Tyre stockpile provides a breeding ground for flies and mosquitoes, this in turn, causing serious diseases (e.g., dengue fever) and affecting human health.
- Large stockpiles cause a fire hazard that could consequently cause uncontrollable burning and air pollution.
- Due to the high cost of legal disposal for solid waste, illegal dumping may increase.
- These wastes take up landfill space. For example, whole tyres are banned from many landfills or are charged higher tipping fees than other waste materials; even if they are carefully buried to prevent them from rising, they are very bulky.

There are a number of options including disposal (in the form of landfill), material recovery and energy recovery [1]. In this study, waste tyre was considered as a precursor in the production of chars, which can be used in removing organics such as phenol [2], dye [3] or heavy metals (e.g., mercury) [4] from wastewater as reported in literature.

Tyre rubber is a mixture of different elastomers such as natural rubber (NB), butadiene rubber (BR) and styrene butadiene rubber (SBR) plus other additives like carbon black, sulphur and zinc oxide. To convert waste tyres into char, a carbonisation (or pyrolysis) process is usually carried out at a relatively low temperature (typically 673–973 K) in the presence of inert gas (e.g., nitrogen, helium or argon) to break down the cross-linkage between carbon atoms. The resultant char characteristics are greatly influenced by the degree of burn-off, which is often a function of temperature, holding time, particle size and heating rate [5–7].

To evaluate the dye adsorption capacity of resultant chars, a series of equilibrium adsorption studies were carried out in which experimental data ($q_{e,experimental}$) were compared with different mathematical descriptions ($q_{e,predicted}$). Non-linear optimisation using sum-of-squared-error (SSE, see Eq. (1)) with the aid of SOLVER add-in by Microsoft® Corporation has been applied to determine the isotherm parameters.

$$SSE = \sum_{i=1} (q_{e,experimental} - q_{e,predicted})_i^2 \quad (1)$$

2. Experimental

2.1. Production of chars

Approximately 100 g of shredded tyre rubber with different particle sizes were pyrolysed in a 18 L muffle furnace (AAF 11/18,

* Corresponding author. Tel.: +852 2358 8412; fax: +852 2358 0054.
E-mail address: kemckayg@ust.hk (G. McKay).

0304-3894/$ – see front matter © 2009 Elsevier B.V. All rights reserved.
doi:10.1016/j.jhazmat.2009.09.142

Nomenclature

a_L	Langmuir isotherm constant (dm^3/mmol)
a_R	Redlich–Peterson isotherm constant [$(dm^3/mmol)^{b_R}$]
a_S	Sips isotherm constant ($(dm^3/mol)^{b_S}$)
a_{TH}	Toth isotherm constant (dm^3/mmol)
b_S	Sips isotherm constant (dimensionless)
b_R	Redlich-Peterson isotherm constant (dimensionless)
B_{TK}	Tempkin isotherm energy constant (dm^3/g)
C	concentration of adsorbate (ppm or mmol/L)
K_F	Freundlich isotherm constant [$(dm^3)^{(1/n_F)}(mmol)^{(1-1/n_F)}$]/g)
K_L	Langmuir isotherm constant (dm^3/g)
K_{TK}	Tempkin isotherm constant (dimensionless)
K_S	Sips isotherm constant [$(dm^3)^{b_S}(mmol)^{1-b_S}$/g]
K_{TH}	Toth isotherm constant (mmol/g)
n_F	Freundlich exponent (dimensionless)
n_{TH}	Toth isotherm exponent (dimensionless)
q_e	amount adsorbed in solid phase (mmol/g)
q_m	monolayer adsorption capacity by Langmuir equation (mmol/g)
SSE	sum-of-squared-error (dimensionless)
ρ_{He}	helium displacement density (g/cc)

Carbolite) under flowing nitrogen (purity 99.99%+, 500 mL/min). In each run, a dried sample was placed in an alumina crucible and heated to the pre-set temperature (473–1173 K) at different heating rates (1–20 K/min), then held isothermal for 1–4 h. The system was allowed to cool in nitrogen until it reached the temperature of 383 K or below. The crucibles were then covered with lids, removed from the furnace and further cooled in a desiccator.

2.2. Characterisation of chars

2.2.1. Surface area and pore size distribution

The surface area and pore size distribution of resultant chars were determined by nitrogen sorption method using Coulter analyser (SA-3100, Coulter). The sample was outgassed at 473 K for 6 h followed by nitrogen sorption at 77 K. The total surface area and micropore volume were determined by BET- and *t*-plot equations, respectively [7]. The total pore volume (i.e., sum of micro- and mesopore volume) is defined as the volume of nitrogen adsorbed at the P/Po ~0.96. Mesopore volume is the difference between total and micropore volume.

2.2.2. Elemental composition and ash content

The elemental analyser (Vario EL III, Varian) was used to determine the carbon, hydrogen, nitrogen and sulphur (CHNS) contents of the sample. By measuring the difference in the electric conductivity between helium reference (ultra-high purity, 99.999%) and reaction gas, the element content of the sample was evaluated. Oxygen content was determined by difference. The ash content of the sample was determined by combustion in a muffle furnace (925 K, 4 h) in accordance with the modified standard test method ASTM D2866-04 [8].

2.2.3. Helium displacement density

An ultrapycnometer (UPY-1000, Quantachrome) was used to measure the helium displacement density (or solid density) of solid. This is accomplished by employing Archimedes' principle and the ideal gas law of fluid displacement. The displaced fluid in this study is helium (ultra-high purity 99.999%) that is able to penetrate into very fine pores or crevices as low as 0.25 nm in diameter. By measuring the volume change before and after helium displacement the true density of the sample can be determined.

Table 1
Basic information of dyes.

	Acid Blue 25	Acid Yellow 117	Methylene Blue
Colour index (CI)	62,055	24,820	52,015
MW (g/mol)	416	848	319
Dye Content (%)	45	60	97
λ_{max} (nm)[a]	600	438	661

[a] Maximum absorbance wavelength.

2.2.4. Equilibrium isotherm

An accurately weighed sample (0.05 g) was added to 50 mL of single-dye solution (Acid Blue 25, Acid Yellow 117 and Methylene Blue, see also Table 1), with different initial concentrations (50–1200 ppm). The sealed bottles were shaken at the speed of 120 rpm for 21 days in a thermostatted shaker at 303 K (Gallenkamp, UK). The mixtures were filtered through syringe filters (0.22 μm, Millex GP, Millipore). After diluting with deionised water, filtrates were analysed by UV–vis spectrophotometer (Cary 1E, Varian).

For comparison, a microporous, commercial carbon (F400) from Calgon® was tested at the same time.

3. Results and discussion

3.1. Effect of temperature

The thermogram in Fig. 1 demonstrates the pyrolysis phenomenon of tyre rubber (particle size 1000–2000 μm) under a nitrogen atmosphere. Pyrolysis initiated at *ca.* 473 K, proceeded vigorously in the temperature interval of *ca.* 593–693 K then stablised at 773 K onward. Increasing the temperature to over 773 K had little effect on the residual mass of tyre rubber as most of the polymeric components in tyre rubber had been converted to gaseous volatiles at temperatures *ca.* 773 K, leaving carbon black as the residue [9–13]. Increasing the pyrolysis temperature from 673 to 1173 K substantially lowered the yield of char from 50.1% at 673 K to 32.3% at 1173 K. This can be explained by a two-step decomposition scheme of SBR, which styrene portion of SBR had not completely decomposed until *ca.* 700 K [14]. Under the same condition the effect of temperature on the elemental composition of chars is tabulated in Table 2.

Progressive aromatisation during a prolonged heating converted hydrocarbons in rubber to lighter gaseous volatiles at higher temperature [15,16]. Higher sulphur and ash contents in char were found, which can be attributed to the reaction between sulphur

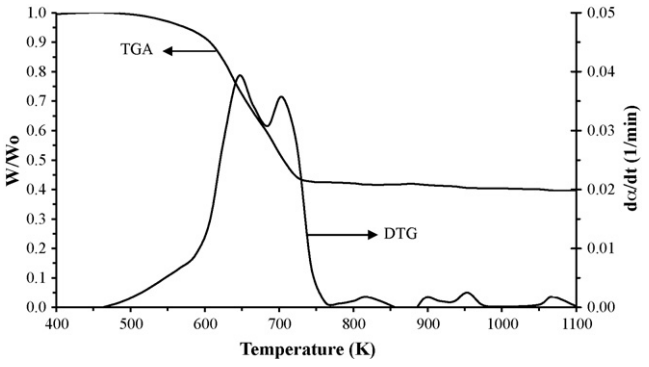

Fig. 1. Thermogravimetric analysis on tyre rubber (heating rate: 5 K/min).

Table 2
Effect of temperature on the elemental composition of chars from tyre rubber.

Temperature (K)	Yield (%)	Elemental composition					Ash (%)
		N	C	S	H	O[a]	
Rubber	–	0.37	81.64	1.95	8.41	0.81	6.82
673	50.10	0.27	80.26	2.44	2.12	7.66	7.25
773	37.15	0.24	81.24	1.67	2.02	5.87	8.96
873	35.43	0.24	81.26	2.33	1.76	4.15	10.26
973	34.93	0.25	83.53	2.51	1.57	1.80	10.34
1073	33.71	0.20	83.27	2.51	0.99	0.07	12.96
1173	32.34	0.21	88.01	2.62	1.02	0.10	8.04

[a] Oxygen content determined by difference.

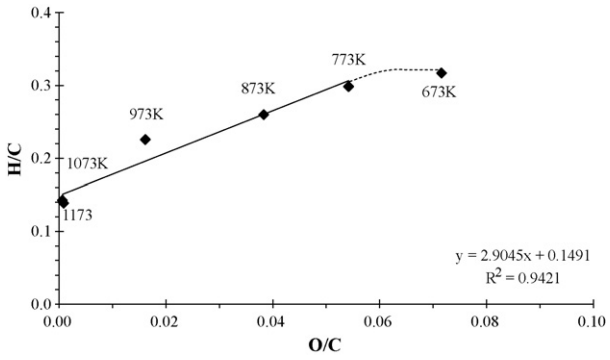

Fig. 2. van Krevelan plot for tyre chars prepared at different temperatures.

and zinc (in the form of ZnO), giving ZnS [17–21] that combined with other minerals in tyre rubber such as Ca, Fe and Si [22] eventually increasing the ash content in the final product. There is an exception at 1173 K, however, as shown in other literature sources [23,24] that the ash contents in tyre char do not necessarily increase with temperature in the range between 923 and 1273 K. This can be attributed to the removal of an organometallic component like Zn at temperature over 773 K [24].

Fig. 2 illustrates the van Krevelen plot for tyre chars prepared at different temperatures under nitrogen. The decreasing H/C following O/C ratios at increasing temperature suggests a growing aromaticity of the char. No significant change in the slope (*ca.* 2.9) of different chars was observed, revealing that the loss of hydrogen from char via dehydrogenation was probably accompanied by a simultaneous conversion of C to CO [25,26]. This agrees with the gaseous product composition, mainly H_2, CO, CO_2 or CH_4 as reported in literature sources [27,28].

Temperature is critical in the porosity development since it is the driving force to the breakdown of linkage between polymeric components, subsequently to the formation of new pores through re-arrangement of carbon atoms [29]. Table 3 shows the effect of pyrolysis temperature on surface area and pore volume (total, micro and meso) of tyre chars in nitrogen for 2 h. The particle size and heating rate were fixed at 1000–2000 μm and 5 K/min, respectively. In a preliminary study, this specific size range gave the highest residual mass fraction (W/W_o) compared with other two tyre rubber fractions of finer particle size (500–710 and 355–500 μm). In addition, it is often preferred to use a lower heating rate to ensure sufficient removal of volatiles during pyrolysis. Therefore 5 K/min was used in attempt to maximise both yield of char and the removal of volatiles evolved in the carbonisation stage.

It is found that the char prepared at 673 K has very limited porosity (10 m^2/g) because the styrene elements in SBR were not decomposed completely at that temperature [30]. When the temperature was raised to 773 K, the decomposition of all polymeric components in tyre rubber has essentially been completed, leaving chars with the surface area and total pore volume the maximum ($S_{BET\text{-}N2}$ 156 m^2/g, V_{total} 0.123 cc/g). Following the continuous release of volatiles and collapse of pore walls due to carbon burn at higher temperature (873 K), more pores were opened and widened which enlarged micropores to mesopores with the mesopore volume 0.178 cc/g. When the temperature was further elevated to 1073 K or above, the pore-widening effect eventually transformed more micropores to mesopores (V_{meso} 0.104 cc/g) even macropores that reduced both surface area and total pore volumes. At the temperature of 1173 K, the surface area and total pore volume were lowered to 87 m^2/g and 0.112 cc/g, respectively with the micropore volume as low as 0.008 cc/g, which contributes to only 7% of the total pore volume.

The helium density of chars only varies in a narrow range between 1.92 g/cc at 673 K to 2.11 g/cc at 1173 K, based on the helium pycnometry measurement which demonstrated a loose structure of chars due to the release of volatiles and agglomeration of carbon black particles at the temperature of over 773 K [11].

3.2. Effect of holding time

Fig. 3 shows the residual mass fraction of tyre rubber with respect to time. The starting temperature (i.e., time = 0) was 378 K and the heating rate was 5 K/min.

The pyrolysis commenced after 20 min (*ca.* 473 K) at which the low boiling point additives such as processing oil and plasticiser were converted to gaseous volatiles [31–33], followed by a sharp weight loss at about 40 min (or *ca.* 593 K), then completed at about 75 min (*ca.* 723 K). The yield and elemental composition of tyre chars prepared 773 K at different holding periods are tabulated in Table 4.

The yield of char is relatively constant in the holding period from 1 to 4 h (average 37.08 ± 1.14%) but decreasing carbon content is observed. It can be attributed to the fixed carbon burn-off due to

Table 3
Effect of temperature on the textural characteristics of chars from tyre rubber.

Temperature (K)	$S_{BET\text{-}N2}$ (m^2/g)	V_{total} (cc/g)	V_{micro} (cc/g)	V_{meso} (cc/g)	ρ_{He} (g/cc)
673	10	0.023	0.000	0.023	1.92
773	156	0.123	0.024	0.099	2.03
873	136	0.193	0.015	0.178	2.09
973	96	0.187	0.013	0.174	2.10
1073	85	0.200	0.008	0.192	2.11
1173	87	0.112	0.008	0.104	2.11

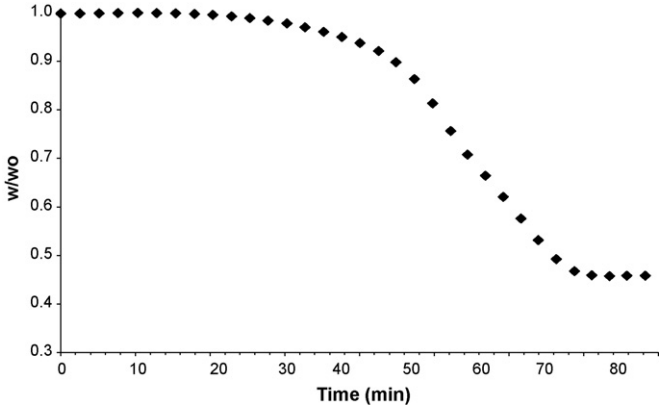

Fig. 3. Residual mass fraction for pyrolysis of tyre rubber with respect to time.

the prolonged heating once the release of volatiles was completed. This also explained the increase of both sulphur and ash contents at longer holding time. The metal content analysis to char pyrolysed at 773 K (Table 5) demonstrated that Zn was the dominant metal which was likely retained in char as ash. Literature [19,24,34,35] further suggested that zinc was likely remained in chars in the form of ZnS, which substantially increased the ash content with other mineral impurities at 773 K.

Table 6 summarises the textural characteristics of chars pyrolysed at different holding time. The surface areas and micropore volumes were found to increase with the holding time, reaching a maximum at 2 h ($S_{BET\text{-}N2}$ 156 m^2/g, V_{micro} 0.024 cc/g) then the values gradually declined to 94 m^2/g and 0.013 cc/g at the point of 4 h. The mesopore volume exhibits a similar trend: it increased steadily from 0.025 cc/g at 1 h to 0.211 cc/g at 3 h then declined to 0.184 cc/g at 4 h. This suggests a continuous widening of pores (both under the isothermal condition which features in the development of mesopores at the expense of micropores (and surface area).

Table 4
Effect of holding time to the elemental composition of chars from tyre rubber (5 K/min, 1000–2000 μm).

Time (h)	Yield (%)	Elemental composition					Ash (%)
		N	C	S	H	O[a]	
1	38.45	0.24	82.39	1.67	1.16	5.68	8.86
2	37.15	0.24	81.24	1.67	1.58	6.34	8.93
3	37.05	0.20	78.55	2.26	1.16	8.88	8.95
4	35.66	0.23	76.50	2.29	1.38	10.36	9.24

[a] Oxygen content determined by difference.

Table 5
Major inorganic species in tyre char pyrolysed at 773 K.

Element	Concentration (mg/kg)
Ca	5,894
Fe	1,329
K	937
Zn	58,539

Table 6
Effect of time on the textural characteristics of tyre chars (773 K, 5 K/min, 1000–2000 μm).

Time (h)	$S_{BET\text{-}N2}$ (m^2/g)	V_{total} (cc/g)	V_{micro} (cc/g)	V_{meso} (cc/g)
1	86	0.033	0.008	0.025
2	156	0.123	0.024	0.099
3	95	0.224	0.013	0.211
4	94	0.197	0.013	0.184

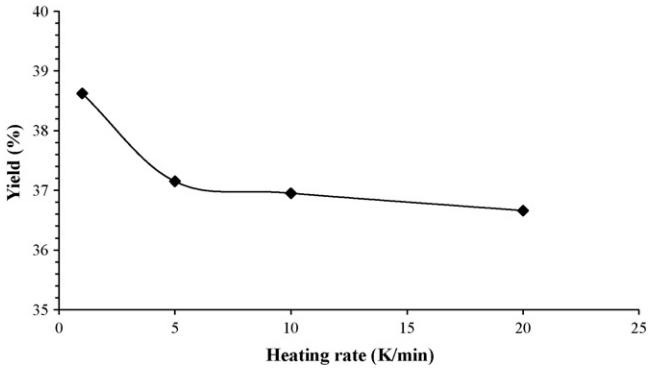

Fig. 4. Effect of heating rate on the yield of char from tyre rubber pyrolysis (N_2, 773 K, 1000–2000 μm, 2 h).

3.3. Effect of heating rate

Fig. 4 shows that char yields generally varied in a narrow range between 36.8% and 38.7% when heating rates increased from 1 to 20 K/min. However, an apparent drop in the char yield at the heating rate of over 1 K/min is observed. The relatively higher yield at 1 K/min can be attributed to the homogeneous heating between particles, which provided sufficient time for secondary reactions between intermediates evolved from polymerisation and condensation [31–33], leaving more carbon deposits onto particles and raising the yield eventually.

This effect further affected the textural characteristics of chars as shown in Table 7, which exhibit a decreasing trend of surface area and pore volumes at increasing heating rates. It has been observed in other biomass pyrolysis studies [36,37]. A similar trend has been reported by Teng et al. [38] in which tyre rubber was pyrolysed in helium at heating rates varied between 3 and 100 K/min. The resultant chars had their surface areas decreased from 98 to 57 m^2/g.

This phenomenon can be explained by the release of volatiles at different heating rates. At the lower heating rate, pyrolysis products have sufficient time to diffuse from the particles. With increasing heating rate the time for the volatiles to be discharged is significantly shortened, leading to an accumulation of volatiles inter- and within particles [36,37]. This may increase the chance of carbon deposits blocking pore entrances, or even similar to coal under high heating rate, which forms blow-holes through which the gaseous volatiles not only can escape but also lead to the collapse of the carbon matrix [38,39] or micropore coalescence [40]. As the consequence of either situation both surface areas and pore volumes were decreased.

3.4. Effect of particle size

As Table 8 demonstrates, the effect of particle size on the yield of char pyrolysed at 773 K is insignificant. This is consistent with other tyre pyrolysis studies which also considered that the particle size effect on pyrolysis is limited [41–44]. It is worthwhile to point out that the carbon content in chars from finer particles is higher. This can be attributed to the tortuous diffusion path between finer particles, which increased the residence time of volatiles involved in secondary reactions [45], leading to the formation of carbon deposits over surface and subsequently raised the carbon content. Senneca et al. [11] further pointed out that carbon black in tyre rubber is likely to act as a nuclei source around which coherent solid carbon grows by cyclisation and/or cross-linking and affects the yields of char. The effect of particle size on the textural characteristics of resultant chars are presented Table 9. Compared with larger size particles (1000–2000 μm), the surface area and pore volumes (micro- and total) of chars from smaller rubber (500–710 μm) are

Table 7
Effect of heating rate on the textural characteristics of tyre chars (773 K, 2 h, 1000–2000 μm).

Heating rate (K/min)	$S_{BET\text{-}N2}$ (m^2/g)	V_{total} (cc/g)	V_{micro} (cc/g)	V_{meso} (cc/g)
1	122	0.079	0.021	0.058
5	156	0.123	0.024	0.099
10	95	0.098	0.010	0.088
20	94	0.030	0.009	0.021

Table 8
Effect of particle size on the elemental composition of tyre chars (773 K, 5 K/min, 2 h).

Particle size (μm)	Yield (%)	Elemental composition					Ash (%)
		N	C	S	H	O[a]	
1000–2000	37.15	0.24	81.24	1.67	1.58	6.34	8.93
500–710	35.15	0.49	88.88	1.40	0.20	1.19	7.84

[a] Oxygen content determined by difference.

Table 9
Effect of particle size on the textural characteristics of tyre chars.

Particle size (μm)	$S_{BET\text{-}N2}$ (m^2/g)	V_{total} (cc/g)	V_{micro} (cc/g)	V_{meso} (cc/g)
1000–2000	156	0.123	0.024	0.099
500–710	117	0.280	0.022	0.258

lower. This is because finer particles have a larger external surface exposed to heat, resulting in an extensive pore-widening thus the surface area and micropore volume decreased as the latter had transformed into mesopores.

3.5. Adsorption isotherms

3.5.1. Acid Blue 25 and Acid Yellow 117

Tyre char prepared at 773 K (2 h) was selected in the adsorption isotherm study. Six isotherm models, namely, Langmuir, Freundlich, Redlich–Peterson, Tempkin, Toth and Sips [46–49], were compared in order to find out and establish the 'best-fit' one. The isotherm parameters for Acid Blue 25 (AB25) and Acid Yellow 117 (AY117) for different models are presented in Tables 10 and 11, respectively.

According to the SSE the Acid Blue 25 adsorption onto tyre char was well-described by the Redlich–Peterson isotherm with the SSE of 6.910×10^{-5}. Both the Toth and Freundlich equations also give similar low SSE values. Fig. 5 also illustrates the fit of the Freundlich isotherm to the experimental data. The very low heterogeneity factor ($1/n_F$) down to 8.075×10^{-2} suggests a highly heterogeneous surface of the tyre char, i.e., $n_F > 2$. The monolayer capacity (q_m), based on the Langmuir analysis, was *ca.* 0.149 mmol/g.

Table 10
Isotherm parameters of Acid Blue 25 adsorption onto tyre char.

Model	Parameters		SSE
Langmuir	K_L	7.996E+01	
	a_L	5.374E+02	3.914E−03
	q_m	1.488E−01	
Freundlich	K_F	1.732E−01	8.690E−05
	$1/n_F$	8.075E−02	
Redlich–Peterson	K_R	2.512E+06	
	a_R	1.497E+07	6.910E−05
	b_R	9.225E−01	
Toth	K_{TH}	1.585E+02	
	a_{TH}	8.362E−02	7.117E−05
	b_{TH}	1.175E−02	
Tempkin	K_{TK}	6.267E+08	2.683E−04
	B_{TK}	7.922E−03	
Sips	K_s	7.996E+01	
	a_s	5.382E+02	3.911E−03
	b_s	1.011E+00	

Table 11
Isotherm parameters of Acid Yellow 117 adsorption onto tyre char.

Model	Parameters		SSE
Langmuir	K_L	4.221E+01	
	a_L	3.822E+02	6.889E−03
	q_m	1.104E−01	
Freundlich	K_F	1.285E−01	7.828E−04
	$1/n_F$	6.736E−02	
Redlich–Peterson	K_R	5.478E+04	
	a_R	4.795E+05	7.609E−04
	b_R	9.634E−01	
Toth	K_{TH}	1.104E+02	
	a_{TH}	8.486E−02	2.271E−03
	b_{TH}	1.230E−02	
Tempkin	K_{TK}	1.129E+10	7.634E−04
	B_{TK}	4.986E−03	
Sips	K_s	2.181E−01	
	a_s	8.419E−01	7.636E−04
	b_s	1.024E+01	

For Acid Yellow 117 (AY117), it was found that the Redlich–Peterson model fitted well to the experimental data

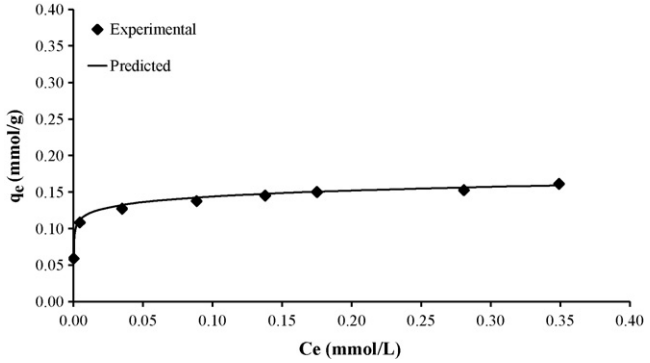

Fig. 5. Equilibrium adsorption isotherm of Acid Blue 25 on tyre char (Best-fit model: Redlich–Peterson).

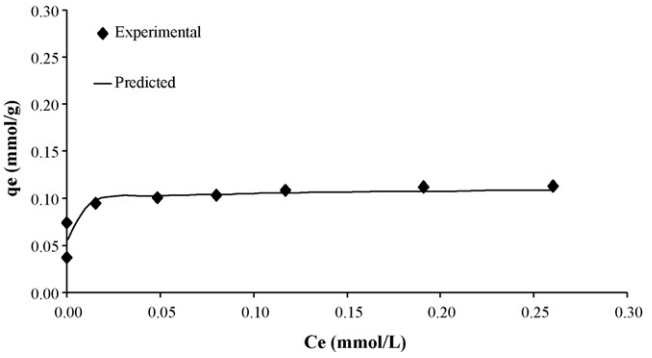

Fig. 6. Equilibrium adsorption isotherm of Acid Yellow 117 on tyre char (Best-fit model: Redlich–Peterson).

based on the SSE value but four other isotherms had similar SSEs. The monolayer capacity of the tyre char was approximately 0.110 mmol/g using the Langmuir equation. This is close to the experimental data using F400 carbon published elsewhere [49]. The experimental and predicted isotherm is shown in Fig. 6.

The difference between the monolayer capacities of the two acidic dyes is mainly due to the molecular size, as the AB25 has a molecular weight nearly half of the AY117 which made the blue dye more favourably adsorbed. However, other factors such as adsorbent pore size distribution, surface charge, molecular orientation, ionic nature or adsorption mechanisms are possible [49,50]. As shown in Table 12 though the surface area of a microporous, commercial carbon (Calgon® F400) is *ca.* 530% higher than tyre char prepared at 773 K (825 versus 156 m^2/g), the amount of Acid Yellow 117 adsorbed onto F400 is *ca.* 38% higher than tyre char, revealing that total surface area is not a sole factor affecting the adsorption capacity. This can be due to the higher mesopore volume in tyre char which allowed better diffusion of the larger sized molecules into inner matrix compared with F400. Similar phenomenon was also observed in different dye–carbon adsorption processes [47,51–53].

3.5.2. Methylene Blue

The adsorption isotherm was determined for a typical basic dye, Methylene Blue, which has a lower molecular weight compared with the two acid dyes in previous section. The optimised isotherm parameters are tabulated in Table 13. From the SSE it suggests that the Sips model provides the best-fit parameters followed by the Toth, Redlich–Peterson and Langmuir. The Langmuir monolayer capacity of the tyre char was 0.405 mmol/g which is comparable to other literature reports [54]. The adsorption isotherm is illustrated in Fig. 7.

Compared with the acid dyes, Methylene Blue has higher affinity to be adsorbed onto tyre char due to two possible factors: smaller molecular weight (319.9 g/mol) of the molecule, which is more likely to diffuse further into inner carbon matrix; and the role of surface charge over carbon surface, which is well understood that is influential to dye adsorption [50,55–57].

Depending on the elemental composition of carbon, the carbon–dye suspension is either acidic or basic, leaving the adsorbent surface positively or negatively charged as postulated below [50]:

$$\text{(negative surface)} \quad C{=}S^{\delta+}OH + H^+ \rightarrow C{=}S^{\delta+} + H_2O \tag{2}$$

$$\text{(Positive surface)} \quad C{=}O^{\delta-}H^+ \rightarrow C{=}O^{\delta-} + H^+ \tag{3}$$

The ionic nature of dye determines the charge of the dissociated molecule in solvents like water. Acid dye with sulphonic groups produces anions while basic dye produces cations. These molecules were found favourably adsorbed onto positively [50,55] and negatively charged carbon surface, respectively [56,57], owing to the electrostatic attraction of opposite charges between adsorbent surface and ions in solution.

Results in Table 14 present the elemental composition of the tyre char and F400. When it is considered together with the amount of Methylene Blue adsorbed in Table 12, the sum of these two elements in tyre char and F400 were 7.9 and 6.0 wt.%, respectively but the amount of the Methylene Blue dye adsorbed by tyre char was about 40% of the F400, even though the latter has much higher surface area (over *ca.* 530%). The higher H and O contents that led

Table 12
Comparison in adsorption capacity by tyre char and F400. .

	$S_{BET\text{-}N2}$ (m^2/g)	q_e (mmol/g)		
		Acid Blue 25	Acid Yellow 117	Methylene Blue
Tyre char	155	0.149	0.110	0.405
F400	825	0.739	0.138	0.932

Table 13
Isotherm parameters of Methylene Blue adsorption onto tyre char.

Model	Parameters		SSE
Langmuir	K_L	3.58E+03	
	a_L	8.84E+03	2.342E−03
	q_m	4.05E−01	
Freundlich	K_F	6.50E−02	4.610E−03
	$1/n_F$	4.02E−01	
Redlich–Peterson	K_R	3.55E+01	
	a_R	8.78E+01	2.340E−03
	b_R	9.98E−01	
Toth	K_{TH}	3.96E−01	
	a_{TH}	5.29E−06	1.594E−03
	b_{TH}	3.76E+00	
Tempkin	K_{TK}	1.29E+07	4.384E−03
	B_{TK}	2.46E−02	
Sips	K_s	1.74E+06	
	a_s	4.41E+06	1.586E−03
	b_s	2.41E−01	

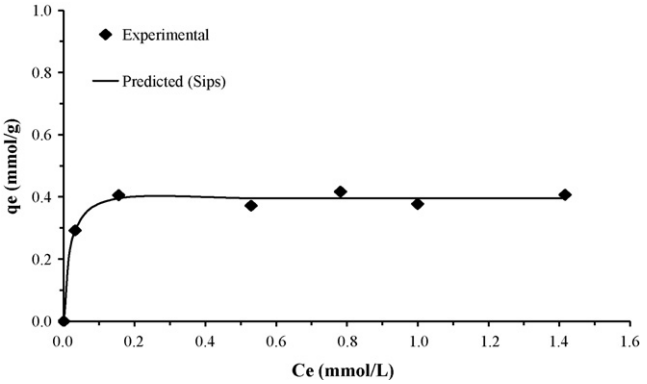

Fig. 7. Equilibrium adsorption isotherm of Methylene Blue on tyre char (Best-fit model: Sips).

Table 14
Comparison in elemental composition of tyre char and F400.

Sample	Elemental composition					Ash (%)	[H + O]
	N	C	S	H	O[a]		
Tyre char	0.24	81.24	1.67	1.58	6.34	8.93	7.92
F400	0.43	87.11	0.72	1.40	4.62	5.72	6.02

[a] Oxygen content determined by difference.

to negatively charged surface of char, in which case more cationic molecules were adsorbed due to the electrostatic attraction.

4. Conclusions

The effect of temperature, holding time, heating rate and particle size to the characteristics of chars prepared from waste tyre were investigated. It is found that, temperature and holding time are the most important factors affecting the yields of chars and surface areas. Significant pore enlargement was observed when pyrolysis temperature increased. Heating rate and particle size are not influential to the yield of chars in both materials but they may affect the textural characteristics of the resultant chars. This is attributed to the temperature gradient of raw materials during pyrolysis, in which the level of shrinkage altered the char structure. Most volatiles were evolved at a temperature of 773 K and increasing the temperature resulted in a higher degree of aromatisation in chars but decreased the yield in return.

In the selection of experimental parameters for pyrolysis all these factors were taken into consideration. The pyrolysis temperature and particle size for waste tyre were fixed at 773 K and 1000–2000 μm, respectively, in order to maximise the surface area of chars. A lower heating rate (e.g., 5 K/min) but longer holding time (e.g., 2 h) are preferred to ensure sufficient removal of volatiles during pyrolysis.

Although the total surface area of a commercial carbon is much higher than the tyre char, the latter exhibited reasonably high adsorption capacity, particularly in the uptake of larger sized molecules such as Acid Yellow 117. This reveals that factors other than total surface area may be involved in the adsorption of specific adsorbate.

Acknowledgements

The authors are grateful to the Research Grant Council (RGC) and Green Island Cement (GIC) for providing the financial support for this research project.

References

[1] P.T. Williams, A.J. Brindle, Temperature selective condensation of tyre pyrolysis oils to maximise the recovery of single ring aromatic compounds, Fuel 82 (2003) 1023–1031.
[2] G. San Miguel, G.D. Fowler, C.J. Sollars, Pyrolysis of tire rubber: porosity and adsorption characteristics of the pyrolytic chars, Ind. Eng. Chem. Res. 37 (1998) 2430–2435.
[3] F. Rozada, M. Otero, A. Moran, A.I. Garcia, Activated carbons from sewage sludge and discarded tyres: production and optimization, J. Hazard. Mater. B124 (2005) 181–191.
[4] E. Manchon-Vizuete, A. Macias-Garcia, A. Nadal Gisbert, C. Fernandez-Gonzalez, V. Gomez-Serrano, Adsorption of mercury by carbonaceous adsorbents prepared from rubber of tyre wastes, J. Hazard. Mater. B119 (2005) 231–238.
[5] J.F. Byrne, H. Marsh, Introductory overview, in: J.W. Patrick (Ed.), Porosity in Carbons: Characterisation and Applications, Halsted Press, New York, 1995, pp. 8–18.
[6] R.T. Yang, Adsorbents: Fundamentals and Applications, John Wiley & Sons, New York, 2003.
[7] J. Rouquerol, K.S.W. Sing, Adsorption by Powders and Porous Solids: Principles, Methodology and Applications, Academic Press, San Diego CA, 1999.
[8] ASTM, Refractories, Carbon and graphite products; activated carbon, in: ASTM (Ed.), Annual Book of ASTM Standards, vol. 15.01, ASTM, Easton, 2005.
[9] P.T. Williams, S. Besler, Pyrolysis-thermogravimetric analysis of tyres and tyre components, Fuel 74 (9) (1995) 1277–1283.
[10] S. Kim, J.K. Park, H.D. Chun, Pyrolysis kinetics of scrap tire rubbers. I: using DTG and TGA, J. Environ. Eng. (1995) 507–514.
[11] O. Senneca, P. Salatino, R. Chirone, A fast heating-rate thermogravimetric study of the pyrolysis of scrap tyres, Fuel 78 (1999) 1575–1581.
[12] Z. Korenova, M. Juma, J. Annus, J. Markos, L. Jelemensky, Kinetics of pyrolysis and properties of carbon black from a scrap tire, Chem. Pap. 60 (6) (2006) 422–426.
[13] S. Galvagno, S. Casu, M. Martino, E. Di Palma, S. Portofino, Thermal and kinetic study of tyre waste pyrolysis via TG-FTIR-MS analysis, J. Thermal. Anal. Calorim. 88 (2) (2007) 507–514.
[14] A. Quek, R. Balasubramanian, An algorithm for the kinetics of tire pyrolysis under different heating rates, J. Hazard. Mater. 166 (2009) 126–132.
[15] R.C. Bansal, J.B. Donnet, H.F. Stoeckli, Active Carbon, Marcel Dekker, New York, 1988.
[16] G. San Miguel, G.D. Fowler, M. Dall-Orso, C.J. Sollars, Porosity and surface characteristic of activated carbons produced from waste tyre rubber, J. Chem. Technol. Biotechnol. 77 (2001) 1–8.
[17] S.Q. Li, Q. Yao, Y. Chi, J.H. Yan, K.F. Cen, Pilot-scale pyrolysis of scrap tires in a continuous rotary kiln reactor, Ind. Eng. Chem. Res. 43 (2004) 5133–5145.
[18] E. Manchon-Vizuete, A. Macıas-Garcıa, A.N. Gisbert, C. Fernandez-Gonzalez, V. Gomez-Serrano, Preparation of mesoporous and macroporous materials from rubber of tyre wastes, Microporous Mesoporous Mater. 67 (2004) 35–41.
[19] A. Chaala, H. Darmstadt, C. Roy, Acid-base method for the demineralization of pyrolytic carbon black, Fuel Process. Technol. 46 (1996) 1–15.
[20] D. Pantea, H. Darmstadt, S. Kaliaguine, C. Roy, Heat-treatment of carbon blacks obtained by pyrolysis of used tires. Effect on the surface chemistry, porosity and electrical conductivity, J. Anal. Appl. Pyrolysis 67 (2003) 55–76.
[21] F. Cataldo, Preparation of pyrolytic carbon black from scrap tire rubber crumb and evaluation in new rubber compounds, Macromol. Mater. Eng. 290 (2005) 463–467.
[22] G. San Miguel, G.D. Fowler, C.J. Sollars, The leaching of inorganic species from activated carbons produced from waste tyre rubber, Water Res. 36 (2002) 1939–1946.
[23] M. Zolezzi, C. Nicolella, S. Ferrara, C. Iacobucci, M. Rovatti, Conventional and fast pyrolysis of automobile shredder residues (ASR), Waste Manage. 24 (7) (2004) 691–699.
[24] J.A. Conesa, I. Martian-Gulloan, R. Font, N.J. Jauhiaine, Complete study of the pyrolysis and gasification of scrap tires in a pilot plant reactor, Environ. Sci. Technol. 38 (2004) 3189–3194.
[25] V. Fierro, V. Torne-Fernandez, A. Celzard, D. Montane, Influence of the demineralisation on the chemical activation of Kraft lignin with orthophosphoric acid, J. Hazard. Mater. 149 (2007) 126–133.
[26] R.K. Sharma, J.B. Wooten, V.L. Baliga, M.R. Hajaligol, Characterization of chars from biomass-derived materials: Pectin chars, Fuel 80 (12) (2001) 1825–1836.
[27] J.F. Gonzalez, J.M. Encinar, J.L. Canito, J.J. Rodriguez, Pyrolysis of automobile tyre waste. Influence of operating variables and kinetics study, J. Anal. Appl. Pyrolysis 58–59 (2001) 667–683.
[28] E. Aylon, A. Fernandez-Colino, M.V. Navarro, R. Murillo, T. Garcia, A.M. Mastral, Waste tire pyrolysis: comparison between fixed bed reactor and moving bed reactor, Ind. Eng. Chem. Res. 47 (2008) 4029–4033.
[29] H. Marsh, F. Rodriguez-Reinoso, Activated Carbon, Elsevier, Amsterdam, 2006.
[30] H. Cui, J. Yang, Z. Liu, Thermogravimetric analysis of two Chinese used tires, Thermochim. Acta 333 (1999) 173–175.
[31] D.Y.C. Leung, C.L. Wang, Kinetic study of scrap tyre pyrolysis and combustion, J. Anal. Appl. Pyrolysis 45 (1998) 153–169.
[32] A. Arion, F. Baronnet, S. Lartiges, J.P. Birat, Characterization of emissions during the heating of tyre contaminated scrap, Chemosphere 42 (2001) 853–859.
[33] C. Diez, M.E. Sanchez, P. Haxaire, O. Martinez, A. Moran, Pyrolysis of tyres: A comparison of the results from a fixed-bed laboratory reactor and a pilot plant (rotatory reactor), J. Anal. Appl. Pyrolysis 74 (2005) 254–258.
[34] L. Tang, H. Huang, An investigation of sulfur distribution during thermal plasma pyrolysis of used tires, J. Anal. Appl. Pyrolysis 72 (2004) 35–40.
[35] H.Y. Lin, W.C. Chen, C.S. Yuan, C.H. Hung, Surface functional characteristics (C, O, S) of waste tire-derived carbon black before and after steam activation, J. Air Waste Manage. Assoc. 58 (1) (2008) 78–84.
[36] A.C. Lua, T. Yang, J. Guo, Effects of pyrolysis conditions on the properties of activated carbons prepared from pistachio-nut shells, J. Anal. Appl. Pyrolysis 72 (2004) 279–287.
[37] A.C. Lua, F.Y. Lau, J. Guo, Influence of pyrolysis conditions on pore development of oil-palm-shell activated carbons, J. Anal. Appl. Pyrolysis 76 (2006) 96–102.
[38] H. Teng, M.A. Serio, M.A. Wojtowicz, R. Bassilakis, P.R. Solomon, Reprocessing of used tires into activated carbon and other products, Ind. Eng. Chem. Res. 34 (1995) 3102–3111.
[39] H.J. Muhlen, K.H. van Heek, Porosity and thermal reactivity, in: J.W. Patrick (Ed.), Porosity in Carbons: Characterisation and Applications, Halsted Press, New York, 1995, pp. 138–148.
[40] M. Guerrero, M. Pilar Ruiz, A. Millera, M.U. Alzueta, R. Bilbao, Characterization of biomass chars formed under different devolatilization conditions: differences between rice husk and eucalyptus, Energy Fuels 22 (2008) 1275–1284.
[41] E. Aylon, M.S. Callen, J.M. Lopez, A.M. Mastral, R. Murillo, M.V. Navarro, S. Stelmach, Assessment of tire devolatilization kinetics, J. Anal. Appl. Pyrolysis 74 (2005) 259–264.
[42] A.M. Cunliffe, P.T. Williams, Influence of process conditions on the rate of activation of chars derived from pyrolysis of used tyres, Energy Fuels 13 (1) (1999) 166–175.
[43] M.M. Barbooti, T.J. Mohamed, A.A. Hussain, F.O. Abas, Optimization of pyrolysis conditions of scrap tires under inert gas atmosphere, J. Anal. Appl. Pyrolysis 72 (2004) 165–170.
[44] M. Olazar, R. Aguado, D. Velez, M. Arabiourrutia, J. Bilbao, Kinetics of scrap tire pyrolysis in a conical spouted bed reactor, Ind. Eng. Chem. Res. 44 (11) (2005) 3918–3924.

[45] M. Rofiqul Islam, H. Haniu, M. Rafigul Alam Beg, Liquid fuels and chemicals from pyrolysis of motorcycle tire waste: product yields, compositions and related properties, Fuel 87 (13–14) (2008) 3112–3122.
[46] S.J. Allen, G. McKay, J.F. Porter, Adsorption isotherm models for basic dye adsorption by peat in single and binary component systems, J. Colloid. Interface Sci. 280 (2004) 322–333.
[47] A.W.M. Ip, J.P. Barford, G. McKay, Production and comparison of high surface area bamboo derived active carbons, Biores. Technol. 99 (18) (2008) 8909–8916.
[48] M.F.F. Sze, V.K.C. Lee, G. McKay, Simplified fixed bed column model for adsorption of organic pollutants using tapered activated carbon columns, Desalination 218 (2008) 323–333.
[49] K.K.H. Choy, J.F. Porter, G. McKay, Single and multicomponent equilibrium studies for the adsorption of acidic dyes on carbon from effluents, Langmuir 20 (2004) 9646–9656.
[50] M. Valix, W.H. Cheung, G. McKay, Roles of the textural and surface chemical properties of activated carbon in the adsorption of acid blue dye, Langmuir 22 (2006) 4574–4582.
[51] Y. Lin, H. Teng, Mesoporous carbons from waste tire char and their application in wastewater discoloration, Microporous Mesoporous Mater. 54 (2002) 167–174.
[52] Y. Al Degs, M.I. El-Barghouthi, M.A. Khraisheh, M.N. Ahmad, S.J. Allen, Effect of surface area, micropores, secondary micropores, and mesopores volumes of activated carbons on reactive dyes adsorption from solution, Sep. Sci. Technol. 39 (1) (2004) 97–111.
[53] S. Lei, J. Miyamoto, H. Kanoh, Y. Nakahigashi, K. Kaneko, Enhancement of the Methylene Blue adsorption rate for ultramicroporous carbon fiber by addition of mesopores, Carbon 44 (2006) 1884–1890.
[54] I.T.S. Garcia, M.R. Nunes, N.L.V. Carreño, W.M. Wallaw, H.V. Fajardo, L.F.D. Probst, Obtenção e Caracterização de Carbono Ativado a partir de Resíduos Provenientes de Bandas de Rodagem, Polímeros: Ciência e Tecnologia 17 (4) (2007) 329–333.
[55] Y. Al Degs, M.A. Khraisheh, S.J. Allen, M.N. Ahmad, Effect of carbon surface chemistry on the removal of reactive dyes from textile effluent, Water Res. 34 (3) (2000) 927–935.
[56] P.C.C. Faria, J.J.M. Orfao, M.F.R. Pereira, Adsorption of anionic and cationic dyes on activated carbons with different surface chemistries, Water Res. 38 (2004) 2043–2052.
[57] M.K. Purkait, A. Maiti, S. Das Gupta, S. De, Removal of congo red using activated carbon and its regeneration, J. Hazard. Mater. 145 (2007) 287–295.